# Run-and-halt behavior of motile droplets in response to light

Alexander Ryabchun, Dhanya Babu, Jacopo Movilli, Rémi Plamont, Nathalie Katsonis*

Stratingh Institute of Chemistry, University of Groningen,
Nijenborgh 7, 9746AG Groningen, The Netherlands

**ABSTRACT**

We report the run-and-halt behavior of motile droplets immersed in an aqueous solution of amphiphilic molecular switch. These oil droplets move autonomously as the switch solubilizes the oil into the water. Droplet movement stops in response to UV light, and picks up again in response to visible light. This motile behavior is a consequence of the reversible *trans*-to-*cis* photo-conversion of the switch in water, because the *trans* photo-isomer stabilizes the oil droplets better than the *cis* photo-isomer, and therefore it also solubilizes the droplet more effectively. Notably, the droplets also evolve positive photokinesis under illumination with visible light, and, in patchy light environments, their complex motility pattern directs the droplets at the periphery of the illuminated areas.

## INTRODUCTION

The ability to move towards light, nutrients and thermal sources plays a vital role in the survival of microorganisms. Unravelling the molecular mechanisms that support the emergence of such purposeful movement in water, including chemotaxis,[1] phototaxis,[2] kinesis,[3] and pathogenesis,[4] requires developing minimalistic analogues. Microscopic motile systems have thus been designed, including liposomes,[5] stomatocytes,[6,7] and other micromotors.[8,9,10,11] Microscopic droplets of oil have also demonstrated chemotactic behavior in aqueous solutions of amphiphiles, [12,13,14] as well as biomimetic motion along helical trajectories.[15,16] These motile droplets move autonomously because the aggregates of amphiphiles present in solution can solubilize small volumes of the oil droplets into water. In this process, the distribution of the amphiphiles at the interface is modified,[17] and the resulting gradient in interfacial tension induces internal and external flows that propel the droplet forward.[18] Pioneering works have shown that the system parameters defining the speed[19], direction,[20] and trajectory[16,21] of the droplets are the concentration and chemical structure of the amphiphile, as well as the size of the motile droplets and the viscosity of the medium in which they move. However, encoding a repertoire of complex behavior remains an ongoing challenge for artificial motile systems.[22]

An essential typical feature of microorganisms is their ability to halt and resume their run. These motile patterns support bacterial search for favorable conditions.[23] For example, *Synechocystis* cyanobacteria adapts its speed to the light intensity, so it can stay longer in regions where the illumination is neither too low nor too strong, and these moderate illumination conditions are favorable to their survival.[24,25] Biomolecular photo-switches are at the origin of this complex behavior: light triggers the all-*trans* isomerization of retinal and this signal is photo-transduced via relay systems, until an enzymatic response eventually halts the movement.

Here, we show that the operation of artificial molecular photo-switches allows encoding complex motility in droplets, including run-and-halt and photokinetic behavior. We use an amphiphilic switch (Azo) and show that the *trans*-Azo isomer sets the droplets in motion while *cis*-Azo stalls the movement (Figure 1). The system also evolves photokinesis, as the speed of the droplets depends on the illumination dose they have received.

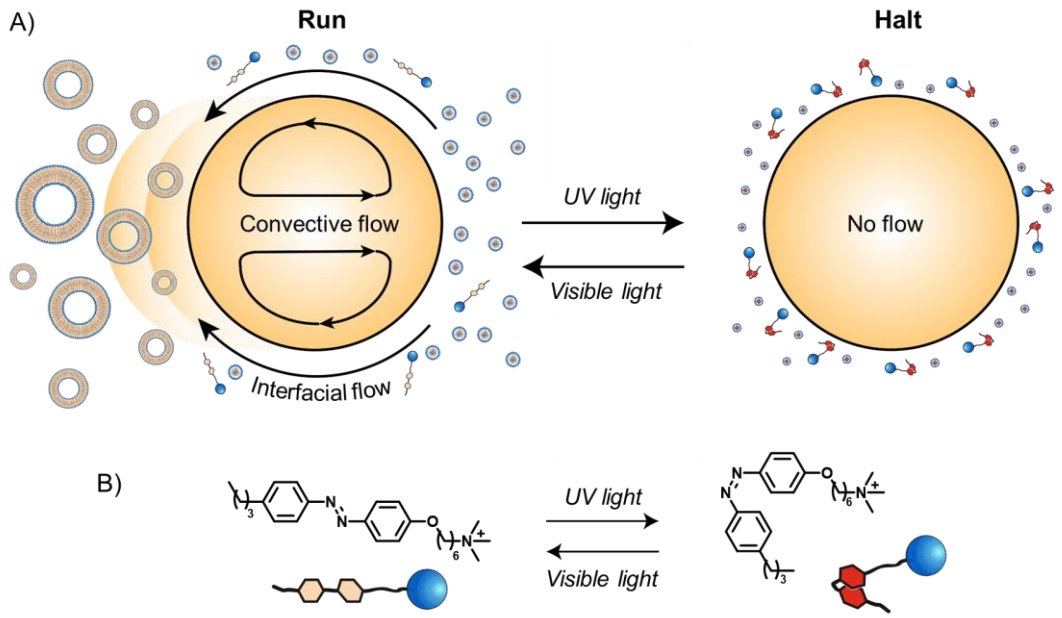


**Figure 1. Run-and-halt behavior of motile droplets in response to light**. A) An oil droplet immersed in an aqueous solution of amphiphilic switch responds to changes in illumination with run-and-halt behavior. B) Reversible photoisomerization of the Azo switch in response to light. Supramolecular aggregates of the *trans*-switch solubilize the droplet into water, thus creating flows that set the droplet in motion. A moving droplet leaves a trail of vesicles, with oil molecules incorporated into their membranes. Upon irradiation with UV light (λ = 365 nm), the switch photo-converts into the *cis*-form, and movement stops. The droplet picks up its run once visible light is switched on again.

## RESULTS AND DISCUSSION

Molecular switches convert light energy into mechanical work,[26,27] and they can develop asymmetry at the interface of the droplets.[28] Azobenzene photoswitches have been used before, to interfere with moving patterns of droplets or solid particles in water.[29,30,31,32] The azobenzene used in our study is functionalized with a hydrophobic tail (the synthetic procedure and characterization are shown in the Supplementary Information, and in Supplementary Figures S1 and S2). This switch undergoes a *trans*-to-*cis* isomerization upon irradiation with UV light ($\lambda = 365$ nm). The back *cis*-to-*trans* conversion occurs spontaneously at room temperature, and can be accelerated by irradiation with visible light (Supplementary Figure S3).[33] The critical micellar concentration of *trans* and *cis* isomers are 0.5 mM and 1.2 mM, respectively (Supplementary Figure S4 and Supplementary Table S1). These values of critical micellar concentration agree with literature reports.[34]

Above a minimal concentration, the switches form micelles that can solubilize small volumes of the oil droplets into water. This solubilization of oil droplets by the switches modifies the interfacial tension of the droplet locally, at random positions, which leads to symmetry breaking events and ultimately propels the droplet forward.[35,36] Liquid crystals are commonly used for the design of motile droplets in water,[36] and here we use a nematic liquid crystal (4′-pentyl-4-biphenylcarbonitrile), hereafter referred to as the oil. Monodisperse droplets of oil were produced using microfluidic devices, with sizes ranging from 35 µm to 185 µm (Supplementary Figure S5). The droplets were transferred to a closed chamber containing the aqueous solution: Milli-Q water in which Azo has been dissolved, and to which $D_2O$ has been added to adjust the density of the aqueous solution to that of the droplets.

In a solution of *trans*-Azo, the droplets move in all directions autonomously (Figure 2A), provided that the concentration of the Azo amphiphile is above a concentration that we call critical propulsion concentration[37] ($CPC_{trans} = 0.8$ mM), which is typically higher than the critical micellar concentration ($CMC_{trans} = 0.5$ mM). We found that increasing the concentration of *trans*-Azo amphiphile leads to an increase in the average speed of the oil droplets because the concentration of micelles that fuel motility increases with the concentration of switch (Figure 2B).

In contrast, the presence of *cis*-Azo in solution does not initiate droplet movement at any concentration, across the entire range. This microscopic behavior has a molecular origin that can be understood from the properties of the amphiphilic switch. C*is* azobenzenes are less compatible with liquid crystalline molecules than *trans* azobenzenes,[38,39] because the bent shape and high dipole moment of the *cis* isomer make it more hydrophilic.[40,41] The *cis* isomer is thus not as effective a surfactant as the *trans* isomer, as confirmed by surface tension measurements (Supplementary Figure S6) and interfacial tension measurements ($\Delta\gamma$ = 15 mN/m, Figure 2C). This difference in surfactant properties is further evidenced by the fact that *trans*-Azo requires to reach a lower critical micellar concentration, before it self-assembles.

When injected in a *trans*-Azo solution, the droplets run in any direction. The droplets stop moving under illumination with UV light, as the switch converts from *trans* to *cis* (Supplementary Video 1 and Supplementary Figure S7). Motility is restored with visible light illumination, which accelerates the *cis*-to-*trans* relaxation. Run-and-halt cycles could be repeated up to six times by alternating illumination with UV and visible light (Figure 2D).

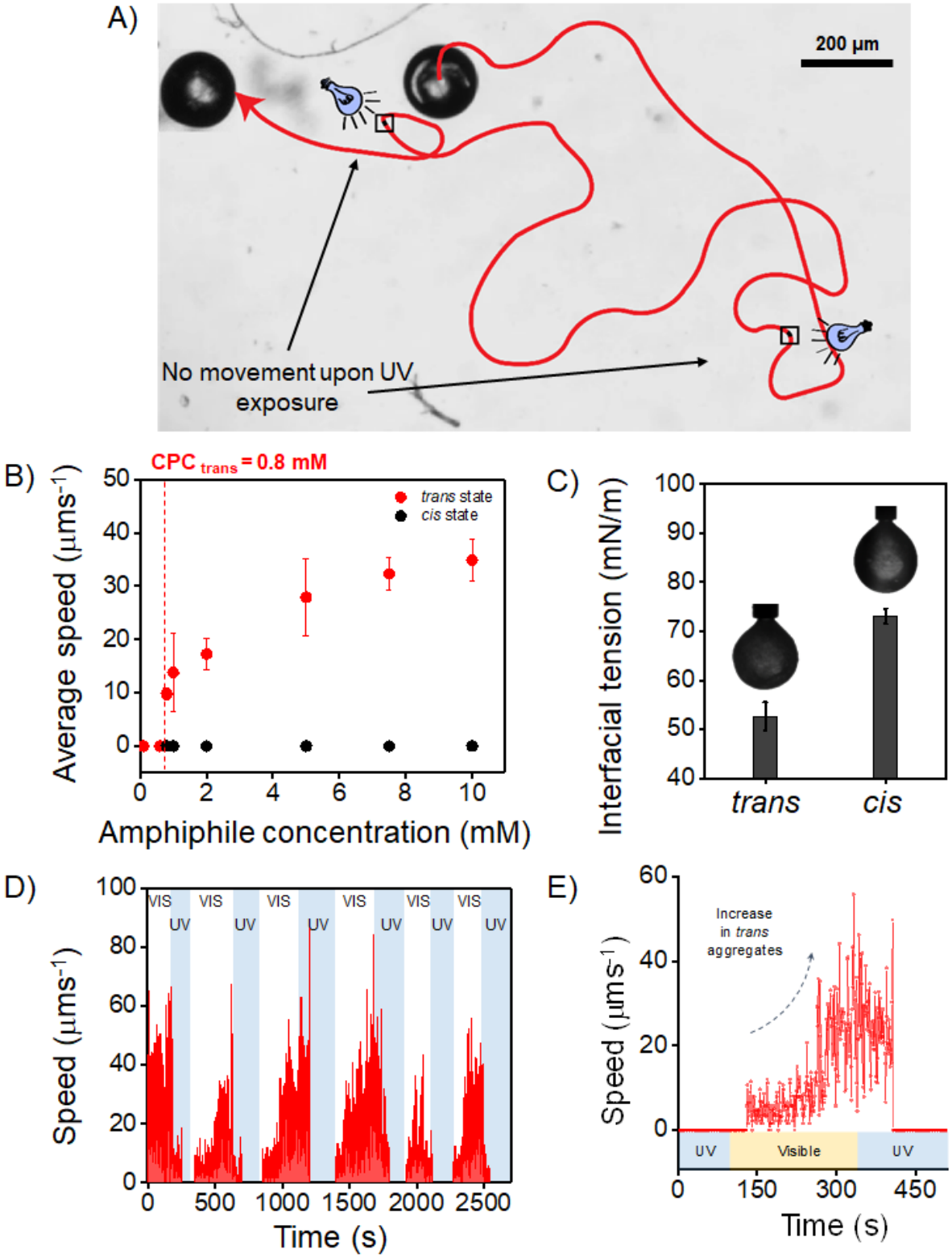


**Figure 2. Run-and-halt behavior of droplets in an aqueous solution of amphiphilic switch.** A) Trajectory of an oil droplet in a 2 mM *trans*-Azo solution in water. The whole trajectory takes 17 min. The black squares pinpoint positions where the droplet halts, as a response to illumination with UV light. Droplet run is resumed by irradiation with visible light. B) Average speed of the droplets with increasing concentration of *trans*-Azo (red) and *cis*-Azo amphiphile

(black). Each data point is an average of five measurements (error bars represent standard deviation). The droplets were ~ 140 µm in diameter. C) Interfacial tension measured at the interface of oil and an aqueous solution of either *trans*-Azo or *cis*-Azo. Measurements were performed at 20°C. D) Run-and-halt behavior can be repeated six times by alternating illumination. Data shown for a 135 µm diameter droplet in a 5 mM Azo solution. E) The droplets accelerate during illumination with visible light. Data shown for a 135 µm diameter droplet in a 5 mM Azo solution.

Systematic size dependent investigations show that the possibility of run-and-halt behavior is dependent on both the diameter of the droplets and Azo concentration in water. Specifically, run-and-halt can be observed for droplets ranging between 30 µm and 180 µm in diameter, under the condition that *trans*-Azo is sufficiently concentrated (Figure 3).

Larger droplets propel faster, which agrees with what is known for chemically-fueled motile droplets, as bigger droplets can maintain a larger gradient of interfacial tension.[42] Upon visible light irradiation, *cis*-to-*trans* conversion allows the active *trans*-isomer to reach critical propulsion concentration, and a gradient in interfacial tension can be formed and sustained, that will make the droplets move.

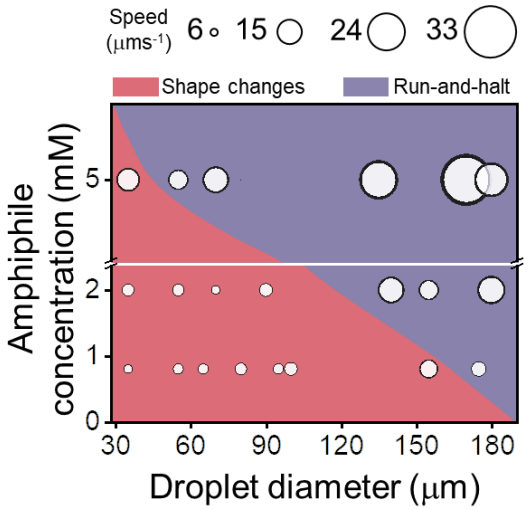


**Figure 3. The motile behavior of the droplets depends on their size and the concentration of the amphiphilic Azo switch.** The purple area corresponds to conditions in which run-and-halt behavior is observed. The pink area corresponds to conditions where run-and-halt behavior is not observed, because the shape of the droplets is not preserved upon *cis*-to-*trans* conversion of the amphiphilic switch. The larger the circles, the faster the droplets.

When the oil droplets are too small, they do not display run-and-halt behavior: they do propel in a *trans*-Azo solution and halt upon *trans*-to-*cis* photo-conversion. However, when irradiated with visible light, they do not pick up movement again, which means that the gradual *cis*-to-*trans* photo-conversion is too slow to induce a substantial gradient of interfacial tension. Instead, the droplets lose their spherical integrity, before the interfacially-active *trans* isomer reaches the minimal concentration that is required for propulsion. Analysis of the droplet speed during run-and-halt behavior shows that the droplets accelerate in the course of illumination with visible light (Figures 2D,E). This acceleration loosely follows the increase in concentration of *trans*-Azo and is analogous to positive photokinesis, in which the speed of microorganisms adapts to changes in the illumination conditions.

In this system, the micelles formed by *trans*-Azo are the fuel for movement. At low concentrations, *trans*-Azo forms spherical micelles with a diameter of ~4.7 nm (Supplementary Figure S8), and at higher concentrations it forms worm-like micelles (Figure 4A). In contrast, *cis*-Azo forms only spherical micelles, with a diameter of ~3.6 nm (Supplementary Figures S8D, S8E, S8F).[43] The diameter of the *cis*-micelles is smaller than that of the *trans*-micelles because the *cis*-switch is shorter than the *trans*-switch (0.9 nm vs 0.5 nm).[44] The fact that both forms of the switch form micelles with different geometries is a signature of their difference in shape and polarity, and constitutes additional evidence for their different effectiveness in solubilizing the oil from the droplets.

Waste is found in the trail of the moving droplets, in the form of giant vesicles (Figure 4). The formation of vesicles was previously observed in systems where a chemical reaction at a droplet interface yields a new vesicular amphiphile,[45] whereas in our system the vesicles are waste material, with a bilayer in which both the *trans*-Azo and the oil removed from the droplet co-exist. These vesicles shrink when irradiated with UV light and eventually they collapse into small oil droplets (Supplementary Figure S9). Such vesicles carrying oil in their bilayer can release oil molecules in response to illumination with UV light, and we anticipate that this mechanism may be exploited for drug delivery purposes.[46]

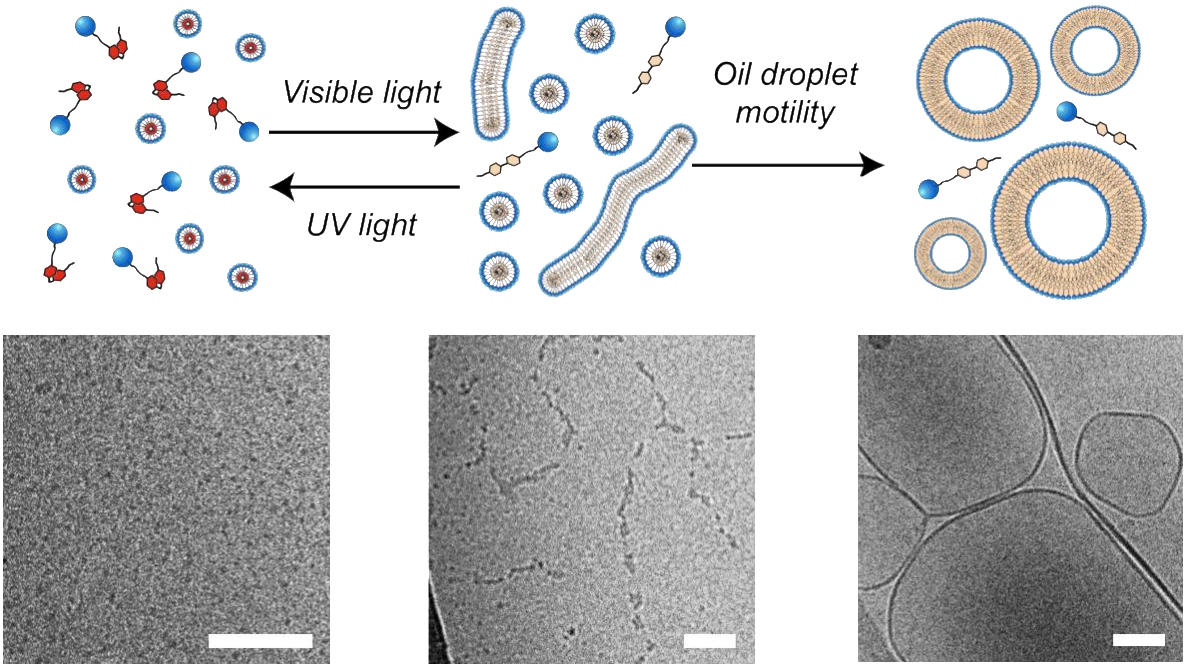


**Figure 4. Supramolecular aggregates of amphiphilic switch drive droplet motion, and giant vesicles are produced as waste.** Cryo-TEM images of *cis*-aggregates (left) and *trans*-aggregates (center) formed in a 7.5 mM Azo solution, in the absence of oil droplets. After droplet movement has occurred, waste vesicles are found in the trail of the droplets (right). Scale bars correspond to 100 nm.

In patchy light environments, positive photokinesis results in accumulation of swimming cells in low light areas.[25] We consequently set off to research the effect of localized irradiation with visible light, on the behavior of a population of droplets. In a circular chamber filled with a solution of *cis*-Azo, the droplets are not moving (Figure 5A and Supplementary Video 2). Upon localized illumination with visible light (λ=455 nm for 10s), a circular area is created, in which there is a high concentration of *trans*-Azo. Illumination with visible light was kept short, to avoid light-driven diffusio-osmosis[47] or chromo-capillary effects.[48] Droplets located within this area started moving actively, while the droplets located far from this area keep stationary (Figure 5A). This observation agrees with the notion that only *trans*-aggregates can act as fuel for droplet motion. We note that thermal effects are negligible here, as the irradiation is short and heat transfer is much faster than diffusion of molecules. A systematic analysis of droplet movement in the area that has been illuminated shows that the droplets are trapped in that circle, with a tendency to remain at the interface with the dark zone (Figure 5A. Stationary droplets that are in the vicinity of the central area that was exposed to visible light, start moving towards it (Figure 5B), after a short lag moment (Supplementary Figure S10). This experiment was

repeated several times (Supplementary Figure S11, and Supplementary Video 3). Overall, we show that patchy illumination with visible light results in the motile droplets accumulating preferentially at the interface between the area that has been illuminated and the area that has stayed in the dark.

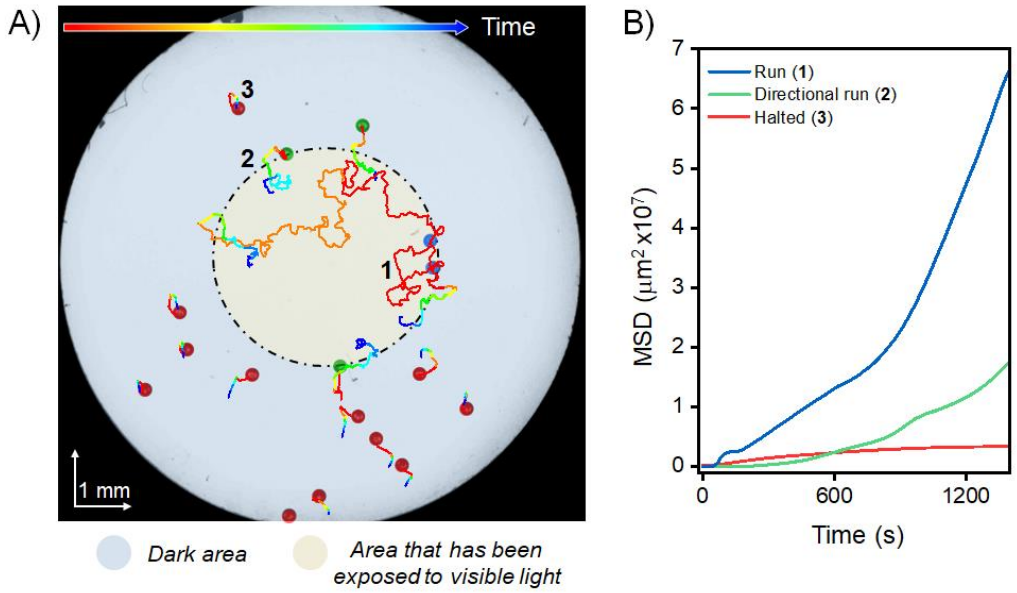


**Figure 5. Motility patterns in patchy conditions of illumination.** A) Optical microscopy image of a chamber showing the initial position of the droplet, and their trajectory during movement. The time scale of the experiment is 114 min. Initially, oil droplets are injected into the chamber filled with *cis*-Azo solution and the chamber is sealed. A circular spot in the chamber, indicated by black dashed line, is then briefly irradiated with visible light (λ = 455 nm), directly through the microscope, and subsequently the video starts. B) Evolution of the mean square displacement in time shows that droplets in the area that has been illuminated start moving shortly after irradiation with visible light has occurred. Outside that zone, droplets move directionally towards the area that has been illuminated, except if they are too far away in the dark zone. Overall, the motile droplets tend to end their motile behavior at the periphery of the illuminated areas.

## CONCLUSION

We show that oil droplets evolve run-and-halt behavior in water, in response to light. The aqueous solution includes an artificial molecular switch that is also an amphiphile, and thus forms micelles in water. Run-and-halt behavior relates to the fact that the two photo-isomers have different interactions with the oil molecules, and, specifically, the *trans*-switch solubilizes

the oil whereas the *cis*-switch does not solubilize the oil in the time frame of the experiments. The propensity of the droplets to display run-and-halt behavior depends on their diameter and the concentration of switchable amphiphile in water. Further, when their environment involves patches of visible light, the droplets accumulate in regions at the interface between the dark areas and those that have been exposed to visible light. Approaches involving artificial molecular motors and switches are both effective in controlling the dynamics of motile systems, and relevant to the study of how purposeful movement can emerge in autonomous minimal compartments. Our findings may thus contribute to an improved understanding for how molecular scale events can translate across length and time scales, into dynamic functionality and useful motion.

## EXPERIMENTAL SECTION

### Production of oil droplets

Monodisperse oil droplets were produced by using a home-made microfluidic device (details can be found in the Supplementary Information). Nematic liquid crystal 4′-pentyl-4-biphenylcarbonitrile (5CB) was purchased from Synthon Chemicals. The oil droplets of 5CB were produced in a 2 wt/v% aqueous solution of polyvinyl alcohol (Sigma). Droplets were produced by using microfluidic chips of different channel sizes [30 μm - 200 μm] and by adjusting the relative flow rates of the oil and aqueous phases.

### Motility experiments

A 60 μL aqueous solution of Azo was introduced into a chamber prepared by attaching a 1 mm-thick silicone film (Electron Microscopy Sciences) with a circular well of 9 mm diameter on a microscopy glass slide. A volume of 6 μL of dispersion containing ≈ 3-5 droplets was then introduced into the chamber. The glass cover was then sealed using a glass cover slip, to prevent evaporation and any external flows affecting the experiment. An Eclipse LV100N POL (Nikon) optical microscope equipped with a DS-Fi3 (Nikon) camera was used to record the videos. All captured videos were analyzed as described in the Supplementary Information.

The sealed chamber was irradiated with UV light (Thorlabs LED, $\lambda$=365 nm, 27.7 mW/cm$^2$) until the droplets stopped propelling. Visible light illumination was provided by the white light of the microscope (3.2 mW/cm$^2$ measured at $\lambda$=455 nm). The light intensity was measured using a PM-100D power meter (Thorlabs) equipped with a thermal power sensor.

For the patchy light environment, a chamber filled with Azo solution was first irradiated with UV light, until the photostationary state was reached. The LED was then switched off, the oil droplets were injected, and the chamber was sealed. Irradiation of the chamber with visible light was performed by shining an LED lamp through the microscope for ~10 s (LED Thorlabs, $\lambda$ = 455 nm, 10.4 mW/cm$^2$), so that there was no need to move the sample. The irradiation area was controlled by the iris field diaphragm of the microscope and was ~3.5 mm in diameter. During observations under the microscope, a low band filter ($\lambda$ < 550 nm) was used to prevent unwanted *cis*-to-*trans* photo-isomerization.

## SUPPLEMENTAL INFORMATION

Supplemental information containing methods, synthesis, and characterization of the azobenzene switch, determination of critical micellar concentration and surface tension, cryo-electron microscopy measurements and image processing can be found online.


## ACKNOWLEDGMENTS

The authors acknowledge funding support from the European Research Council (ERC Consolidator Grant Morpheus 772564). D.B. is supported by the curiosity-driven research program ECHO (712.017.003) which is financed by the Dutch Research Council (NWO). R. P. acknowledges the Volkswagen Foundation for financial support (Integration of Molecular Components in Functional Macroscopic Systems, 93424). We thank Dr. Marc Stuart for technical assistance and for sharing his expertise on electron microscopy.


## AUTHOR INFORMATION


### Corresponding Author

*E-mail: n.h.katsonis@rug.nl

### ORCID

Alexander Ryabchun: 0000-0001-9605-3067

Dhanya Babu: 0000-0002-2783-6241

Jacopo Movilli: 0000-0001-6691-0654

Rémi Plamont : 0000-0002-9024-3254

Nathalie Katsonis : 0000-0003-1054-6544


## DECLARATION OF INTERESTS

The authors declare no competing financial interest.

# 1 REFERENCES


1. Porter, S.L., Wadhams, G.H., and Armitage, J.P. (2011). Signal processing in complex chemotaxis pathways. Nat. Rev. Microbiol. *9*, 153–165.

2. Bhaya, D. (2004). Light matters: phototaxis and signal transduction in unicellular cyanobacteria. Mol. Microbiol. *53*, 745–754.

3. Choi, J.S., Chung, Y.H., Moon, Y.J., Kim, C., Watanabe, M., Song, P.S., Joe, C.O., Bogorad, L., and Park, Y.M. (1999). Photomovement of the gliding cyanobacterium Synechocystis. Photochem. Photobiol. *70*, 95–102.

4. Wilson, J.W., Schurr, M.J., LeBlanc, C.L., Ramamurthy, R., Buchanan, K.L., and Nickerson, C.A. (2002). Mechanisms of bacterial pathogenicity. Postgrad. Med. J. *78*, 216–224.

5. Somasundar, A., Ghosh, S., Mohajerani, F., Massenburg, L.N., Yang, T., Cremer, P.S., Velegol, D., and Sen, A. (2019). Positive and negative chemotaxis of enzyme-coated liposome motors. Nat. Nanotechnol. *14*, 1129-1134.

6. Wilson, D.A., Nolte, R.J.M., and van Hest, J.C.M. (2012). Autonomous movement of platinum-loaded stomatocytes. Nat. Chem. *4*, 268–274.

7. Shao, J., Cao, S., Williams, D.S., Abdelmohsen, L.K.E.A., and van Hest, J.C.M. (2020). Photoactivated polymersome nanomotors: Traversing biological barriers. Angew. Chem. Int. Ed. *59*, 16918–16925.

8. Wang, L., Song, S., van Hest, J., Abdelmohsen, L.K.E.A., Huang, X., and Sánchez, S. (2020). Biomimicry of cellular motility and communication based on synthetic soft-architectures. Small *16*, 1–19.

9. Vicario, J., Eelkema, R., Browne, W.R., Meetsma, A., La Crois, R.M., and Feringa, B.L. (2005). Catalytic molecular motors: Fuelling autonomous movement by a surface bound synthetic manganese catalase. Chem. Commun., 3936–3938.

10. Brooks, A.M., Tasinkevych, M., Sabrina, S., Velegol, D., Sen, A., and Bishop, K.J.M. (2019). Shape-directed rotation of homogeneous micromotors via catalytic self-electrophoresis. Nat. Commun. *10*, 1–9.

11. Doherty, R.P., Varkevisser, T., Teunisse, M., Hoecht, J., Ketzetzi, S., Ouhajji, S., and Kraft, D.J. (2020). Catalytically propelled 3D printed colloidal microswimmers. Soft Matter *16*, 10463–10469.

12. Maass, C.C., Krüger, C., Herminghaus, S., and Bahr, C. (2016). Swimming droplets. Annu. Rev. Condens. Matter Phys. *7*, 171–193.

13. Jin, C., Krüger, C., and Maass, C.C. (2017). Chemotaxis and autochemotaxis of self-propelling droplet swimmers. Proc. Natl. Acad. Sci. U. S. A. *114*, 5089–5094.

14. Meredith, C.H., Moerman, P.G., Groenewold, J., Chiu, Y.J., Kegel, W.K., van Blaaderen, A., and Zarzar, L.D. (2020). Predator–prey interactions between droplets driven by non-reciprocal oil exchange. Nat. Chem. *12*, 1136–1142.

15. Yamamoto, T., and Sano, M. (2017). Chirality-induced helical self-propulsion of cholesteric liquid crystal droplets. Soft Matter *13*, 3328–3333.

16. Krüger, C., Klös, G., Bahr, C., and Maass, C.C. (2016). Curling liquid crystal microswimmers: A cascade of spontaneous symmetry breaking. Phys. Rev. Lett. *117*, 048003.

17. Izri, Z., van der Linden, M.N., Michelin, S., and Dauchot, O. (2014). Self-propulsion of pure water droplets by spontaneous marangoni-stress-driven motion. Phys. Rev. Lett. *113*, 1–5.

18. Schmitt, M., and Stark, H. (2016). Marangoni flow at droplet interfaces: Three-dimensional solution and applications. Phys. Fluids *28*, 012106.

19. Thutupalli, S., Seemann, R., and Herminghaus, S. (2011). Swarming behavior of simple model squirmers. New J. Phys. *13*, 073021.

20. Jin, C., Hokmabad, B. V., Baldwin, K.A., and Maass, C.C. (2018). Chemotactic droplet swimmers in complex geometries. J. Phys. Condens. Matter *30*, 054003.

21. Dwivedi, P., Pillai, D., and Mangal, R. (2020). Solute induced chaotic motion of self-propelled droplets. arXiv, 13–16.

22. Lancia, F., Yamamoto, T., Ryabchun, A., Yamaguchi, T., Sano, M., and Katsonis, N. (2019). Reorientation behavior in the helical motility of light-responsive spiral droplets. Nat. Commun. *10*, 2–9.

23. Lauga, E. (2016). Bacterial hydrodynamics. Annu. Rev. Fluid Mech. *48*, 105–130.

24. Chung, Y.H., Park, Y.M., Moon, Y.J., and Lee, E.M., Choi, J.S. (2004). Photokinesis of cyanobacterium synechocystis. J. Photosci. *11*, 89–94.

25. Wilde, A., and Mullineaux, C.W. (2017). Light-controlled motility in prokaryotes and the problem of directional light perception. FEMS Microbiol. Rev. *41*, 900–922.

26. van Leeuwen, T., Lubbe, A.S., Štacko, P., Wezenberg, S.J., and Feringa, B.L. (2017). Dynamic control of function by light-driven molecular motors. Nat. Rev. Chem. *1*, 1–7.

27. Lancia, F., Ryabchun, A., and Katsonis, N. (2019). Life-like motion driven by artificial molecular machines. Nat. Rev. Chem. *3*, 536–551.

28. Zhang, D., Sun, Y., Li, M., Zhang, H., Song, B., and Dong, B. (2018). A phototactic liquid micromotor. J. Mater. Chem. C *6*, 12234–12239.

29. Liu, X., and Abbott, N.L. (2009). Spatial and temporal control of surfactant systems. J. Colloid Interface Sci. *339*, 1–18.

30. Xiao, Y., Zarghami, S., Wagner, K., Wagner, P., Gordon, K.C., Florea, L., Diamond, D., and Officer, D.L. (2018). Moving droplets in 3D using light. Adv. Mater. *30*, 1–8.

31. Florea, L., Wagner, K., Wagner, P., Wallace, G.G., Benito-Lopez, F., Officer, D.L., and Diamond, D. (2014). Photo-chemopropulsion-light-stimulated movement of microdroplets. Adv. Mater. *26*, 7339–7345.

32. Kaneko, S., Asakura, K., and Banno, T. (2017). Phototactic behavior of self-propelled micrometer-sized oil droplets in a surfactant solution. Chem. Commun. *53*, 2237–2240.

33. Arya, P., Jelken, J., Lomadze, N., Santer, S., and Bekir, M. (2020). Kinetics of photo-isomerization of azobenzene containing surfactants. J. Chem. Phys. *152*, 024904.

34. Arya, P., Jelken, J., Feldmann, D., Lomadze, N., and Santer, S. (2020). Light driven diffusioosmotic repulsion and attraction of colloidal particles. J. Chem. Phys. *152*, 194703.

35. Kovalchuk, N.M., and Vollhardt, D. (2006). Marangoni instability and spontaneous non-linear oscillations produced at liquid interfaces by surfactant transfer. Adv. Colloid Interface Sci. *120*, 1–31.

36. Herminghaus, S., Maass, C.C., Krüger, C., Thutupalli, S., Goehring, L., and Bahr, C. (2014). Interfacial mechanisms in active emulsions. Soft Matter *10*, 7008–7022.

37. Babu, D., Scanes, R., Plamont, R., Ryabchun, A., Lancia, F., Kudernac, T., Fletcher, S.P., and Katsonis, N. (2021). Acceleration of lipid reproduction by emergence of microscopic motion. Nat. Commun., *accepted for publication*.

38. Gelebart, A.H., Liu, D., Mulder, D.J., Leunissen, K.H.J., van Gerven, J., Schenning, A.P.H.J., and Broer, D.J. (2018). Photoresponsive sponge-like coating for on-demand liquid release. Adv. Funct. Mater. *28*, 1–8.

39. Lancia, F., Ryabchun, A., Nguindjel, A.D., Kwangmettatam, S., and Katsonis, N. (2019). Mechanical adaptability of artificial muscles from nanoscale molecular action. Nat. Commun. *10*, 1–8.

40. Zakrevskyy, Y., Roxlau, J., Brezesinski, G., Lomadze, N., and Santer, S. (2014). Photosensitive surfactants: Micellization and interaction with DNA. J. Chem. Phys. *140*, 01B612_1.

41. Lin, Y., Cheng, X., Qiao, Y., Yu, C., Li, Z., Yan, Y., and Huang, J. (2010). Creation of photo-modulated multi-state and multi-scale molecular assemblies via binary-state molecular switch. Soft Matter *6*, 902–908.

42. Ueno, N., Banno, T., Asami, A., Kazayama, Y., Morimoto, Y., Osaki, T., Takeuchi, S., Kitahata, H., and Toyota, T. (2017). Self-propelled motion of monodisperse underwater oil droplets formed by a microfluidic device. Langmuir *33*, 5393–5397.

43. Blayo, C., Houston, J.E., King, S.M., and Evans, R.C. (2018). Unlocking structure-self-assembly relationships in cationic azobenzene photosurfactants. Langmuir *34*, 10123–10134.

44. Montagna, M., and Guskova, O. (2018). Photosensitive cationic azobenzene surfactants: Thermodynamics of hydration and the complex formation with poly(methacrylic acid). Langmuir *34*, 311–321.

45. Toyota, T., Tsuha, H., Yamada, K., Takakura, K., Ikegami, T., and Sugawara, T. (2006). Listeria-like motion of oil droplets. Chem. Lett. *35*, 708–709.

46. Kauscher, U., Holme, M.N., Björnmalm, M., and Stevens, M.M. (2019). Physical stimuli-responsive vesicles in drug delivery: Beyond liposomes and polymersomes. Adv. Drug Deliv. Rev. *138*, 259–275.

47. Feldmann, D., Maduar, S., Santer, M., Lomadze, N., Vinogradova O.I., and Santer, S. (2016). Manipulation of small particles at solid liquid interface: light driven diffusioosmosis. Sci Rep *6*, 36443.

48. Diguet, A., Guillermic, R-M., Magome, N., Saint-Jalmes, A., Chen, Y., Yoshikawa, K., and Baigl, D. (2009). Photomanipulation of a droplet by the chromocapillary effect. Angew. Chem. Int. Ed. *48*, 9281–9284.